SMC-TR-92-41

AEROSPACE REPORT NO.
TR-0091(6945-03)-2

Surface Phonon Dispersion of MoS_2

Prepared by

P. A. BERTRAND
Mechanics and Materials Technology Center
Technology Operations

31 July 1992

Prepared for

SPACE AND MISSILE SYSTEMS CENTER
AIR FORCE MATERIEL COMMAND
Los Angeles Air Force Base
P. O. Box 92960
Los Angeles, CA 90009-2960

Contract No. F04701-88-C-0089

Engineering and Technology Group

THE AEROSPACE CORPORATION
El Segundo, California

This report was submitted by The Aerospace Corporation, El Segundo, CA 90245-4691, under Contract No. F04701-88-C-0089 with the Space and Missile Systems Center, P.O. Box 92960-4691, Los Angeles, CA 90009-2960. It was reviewed and approved for The Aerospace Corporation by R. W. Fillers, Principal Director, Mechanics and Materials Technology Center. Captain Mark Borden was the project officer for the Mission-Oriented Investigation and Experimentation program.

This report has been reviewed by the Public Affairs Office (PAS) and is releasable to the National Technical Information Service (NTIS). At NTIS, it will be available to the general public, including foreign nationals.

This technical report has been reviewed and is approved for publication. Publication of this report does not constitute Air Force approval of the report's findings or conclusions. It is published only for the exchange and stimulation of ideas.

QUANG BUI, Lt., USAF
MOIE Program Manager

MARK W. BORDEN, Captain, USAF
SSUSI/SSULI Project Officer
DMSP Program Office

UNCLASSIFIED

SECURITY CLASSIFICATION OF THIS PAGE

REPORT DOCUMENTATION PAGE

1a. REPORT SECURITY CLASSIFICATION Unclassified	1b. RESTRICTIVE MARKINGS
2a. SECURITY CLASSIFICATION AUTHORITY	3. DISTRIBUTION/AVAILABILITY OF REPORT Approved for public release; distribution unlimited
2b. DECLASSIFICATION/DOWNGRADING SCHEDULE	
4. PERFORMING ORGANIZATION REPORT NUMBER(S) TR-0091(6945-03)-2	5. MONITORING ORGANIZATION REPORT NUMBER(S) SMC-TR-92-41
6a. NAME OF PERFORMING ORGANIZATION The Aerospace Corporation Technology Operations 6b. OFFICE SYMBOL *(If applicable)*	7a. NAME OF MONITORING ORGANIZATION Space and Missile Systems Center
6c. ADDRESS *(City, State, and ZIP Code)* El Segundo, CA 90245-4691	7b. ADDRESS *(City, State, and ZIP Code)* Los Angeles Air Force Base Los Angeles, CA 90009-2960
8a. NAME OF FUNDING/SPONSORING ORGANIZATION 8b. OFFICE SYMBOL *(If applicable)*	9. PROCUREMENT INSTRUMENT IDENTIFICATION NUMBER F04701-88-C-0089
8c. ADDRESS *(City, State, and ZIP Code)*	10. SOURCE OF FUNDING NUMBERS PROGRAM ELEMENT NO. / PROJECT NO. / TASK NO. / WORK UNIT ACCESSION NO.

11. TITLE *(Include Security Classification)*
Surface Phonon Dispersion of MoS_2

12. PERSONAL AUTHOR(S)
Bertrand, P. A.

13a. TYPE OF REPORT	13b. TIME COVERED	14. DATE OF REPORT *(Year, Month, Day)*	15. PAGE COUNT
	FROM _____ TO _____	1992 July 31	23

16. SUPPLEMENTARY NOTATION

17. COSATI CODES		
FIELD	GROUP	SUB-GROUP

18. SUBJECT TERMS *(Continue on reverse if necessary and identify by block number)*
Molybdenumdisulfide
Surface vibrational spectroscopy
Electron energy loss spectroscopy
Layer-lattice compounds

19. ABSTRACT *(Continue on reverse if necessary and identify by block number)*

The dispersion of phonons on the (0001) surface of MoS_2 was measured by high-resolution electron energy loss spectroscopy along both the <010> and <110> azimuths (i.e., Γ to K and Γ to M, respectively). The surface phonons have lower energies than the corresponding bulk phonons, which indicates that the bonding interactions of the surface atoms are different from those of the bulk, even in a layer lattice compound. Since sputtered MoS_2 lubricant films are composed of many small crystallites, the relative number of surface atoms in a film is much higher than in a single crystal. The stronger bonding of the surface layer may affect the amount of inter- vs intra-crystalline slip in the lubrication mechanism. This work also demonstrates the use and usefulness of a new technique (high-resolution electron energy loss spectroscopy) in this laboratory.

20. DISTRIBUTION/AVAILABILITY OF ABSTRACT	21 ABSTRACT SECURITY CLASSIFICATION
☒ UNCLASSIFIED/UNLIMITED ☐ SAME AS RPT. ☐ DTIC USERS	Unclassified
22a. NAME OF RESPONSIBLE INDIVIDUAL	22b. TELEPHONE *(Include Area Code)* / 22c. OFFICE SYMBOL

DD FORM 1473, 84 MAR 83 APR edition may be used until exhausted. All other editions are obsolete

SECURITY CLASSIFICATION OF THIS PAGE

UNCLASSIFIED

CONTENTS

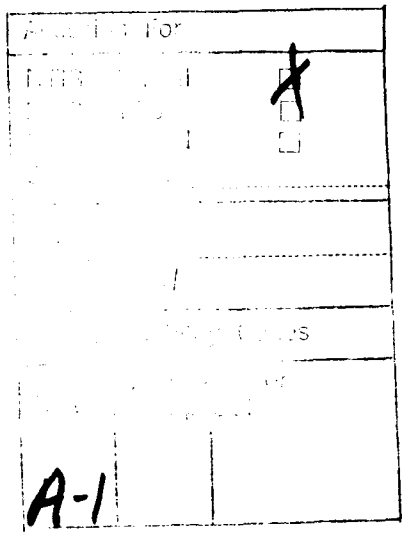

FIGURES

TABLE

I. INTRODUCTION

The surface properties of layered materials such as graphite and the chalcogenides MoS_2 and GaSe are a subject of much interest. Within each layer, strong covalent bonding prevails; however, only weak van der Waals interactions are operative between layers. To a first approximation, the surface properties of such materials might be thought of as identical to the bulk properties. For instance, the (0001) surfaces of MoS_2, $NbSe_2$, and GaSe show 1 x 1 LEED patterns, indicative of no major surface reconstruction. A careful study of the LEED intensities for MoS_2 and $NbSe_2$ indicates a contraction of less than 5% of the first van der Waals gap in MoS_2, and no changes in $NbSe_2$ (Ref. 1).

The dispersion of surface phonons in graphite has been measured by high-resolution electron energy loss spectroscopy (HREELS) (Refs. 2, 3) and is considered to be similar to that of the bulk phonons as measured by neutron scattering (Ref. 4). Inelastic He scattering was used to measure the surface phonon dispersion of GaSe (Ref. 5), where large differences from the bulk phonon dispersion were observed. The lower surface phonon energies were attributed to lower force constants and higher polarizability of Se at the surface, causing increased van der Waals attraction.

In this report, we describe the surface phonon dispersion of MoS_2 measured by HREELS. The crystal structure of MoS_2 is illustrated in Figure 1a. Each S-Mo-S sandwich is tightly bound internally and interacts with neighboring sandwiches only through van der Waals forces. Figure 1b shows projections of the MoS_2 unit cell on the (110) plane and the (0001) (basal) plane, and the conventional surface Brillouin zone with the high symmetry points marked is shown in Figure 1c. In the experiments reported here, the surface phonons are found to be lower in energy than the bulk phonons, as in the case of GaSe, indicating differences between the bonding in the topmost layer and the bulk layers.

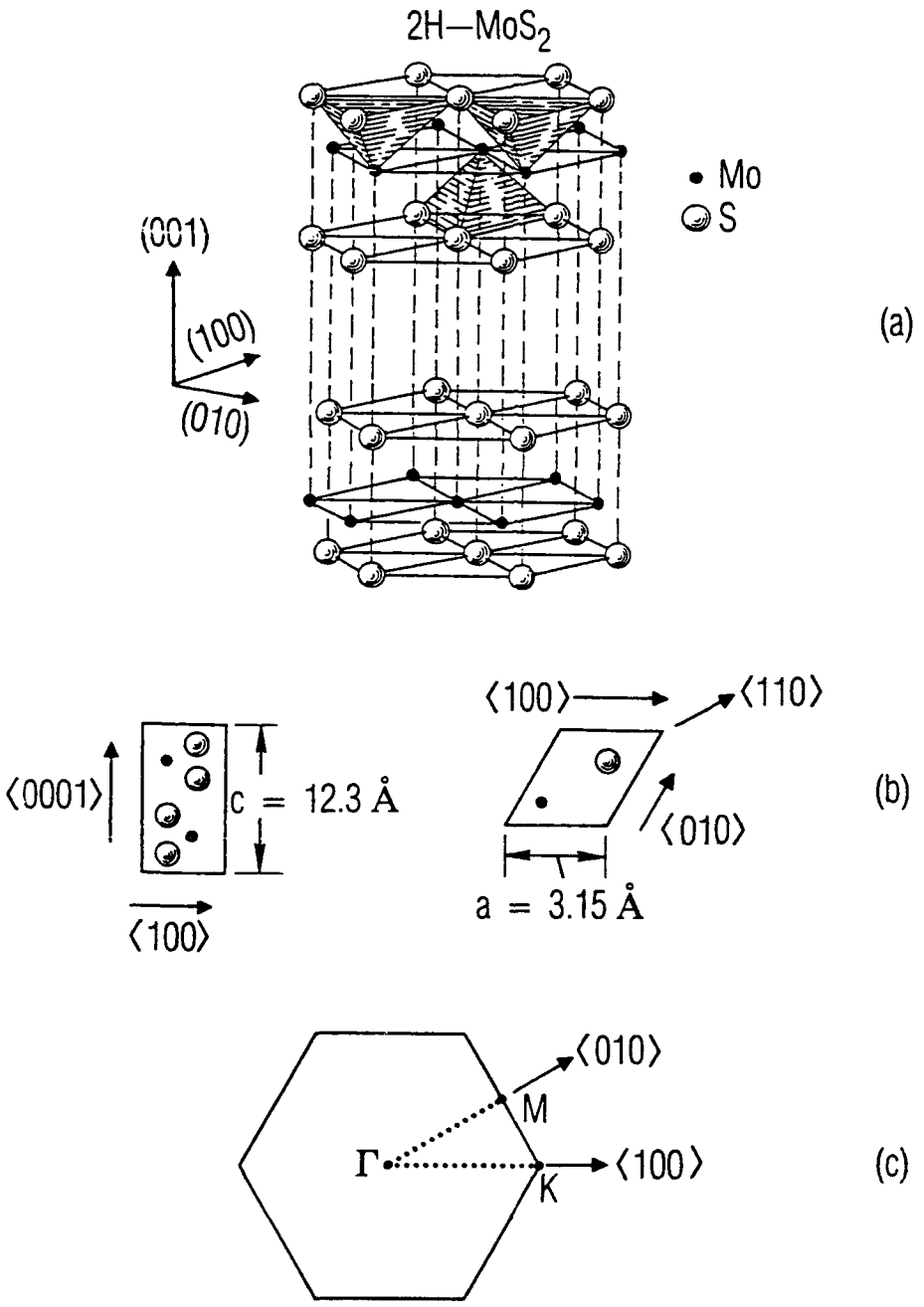

Figure 1. (a) Crystal structure of MoS_2, (b) unit cell of MoS_2, and (c) surface Brillouin zone of MoS_2.

II. EXPERIMENTAL

Basal plane surfaces of MoS_2 were produced by cleavage in air of natural molybdenite crystals (supplied by Ward's Natural Science Establishment, Rochester, NY). The samples were cleaned by heating to 750 K for 10 min at 10^{-10} torr to drive off adsorbed hydrocarbons. This procedure removes virtually all contaminants without producing defects (Ref. 6). HREELS spectra before cleaning showed only hydrocarbon contaminant vibrations; after cleaning, only those due to MoS_2 were present. Good quality (0001) 1 x 1 LEED patterns were obtained and used to orient the sample along the <010> or <110> azimuths for the dispersion measurements.

The spectra were taken with a double pass spectrometer (LK 2000 from LK Technologies, Inc.) with a sample current of $\sim 10^{-10}$ A and a resolution of 9 meV for the MoS_2 samples used here. A resolution of 6 meV has been obtained by biasing the sample so that the electrons are reflected from a smooth electric field above the sample, but a real surface with contaminants and defects will have a poorer resolution. Spectra were collected digitally and typically took 1.5 hr each. The angle of incidence of the electrons was fixed at 60° with respect to the surface normal, and the angle of collection of the scattered electrons was varied from 60° (specular reflection) to 27° with respect to the surface normal to collect electrons of the desired momentum transfer. Spectra were collected with incident beam energies of 7, 15, 30, and 40 eV. In some cases the sample was cooled to 120 K to reduce the intensity of phonon deexitation peaks ("gain" peaks).

III. RESULTS

Typical spectra for 15 eV incident beam energy are shown in Figure 2 (along Γ to M) and Figure 3 (along Γ to K). Optical phonons near 50 meV are present in specular reflection and, as the momentum transfer is increased, additional vibrations begin to appear near the elastic peak. The same general observations can be made for the spectra taken with other beam energies; the phonon peaks are less intense for the 30 and 40 eV incident beams. Overtones of the vibrations can be observed at twice the phonon energy, but are so low in intensity that they cannot be used in the analysis.

The overlap of the peaks makes location of the peak positions difficult, and a curve-fitting procedure was used. The overlapping peaks were represented by Gaussians of half-width 9 meV (the half-width of the elastic peak at k = 0). This half-width was used for all the peaks in the absence of any compelling reason for allowing it to vary, in order to reduce the number of adjustable parameters used in the curve fitting. The phonon creation and annihilation (loss and gain) peaks were equally spaced on each side of the elastic peak, and were given an intensity ratio appropriate to the temperature of the measurement:

$$I_g = I_l \, e^{-E/kT}$$

where I_g and I_l are the intensities of the gain and loss peaks, respectively, E is the energy of the phonon, k is the Boltzmann constant, and T is the temperature. The position and amplitude of the elastic and loss peaks were then varied to produce the best fit to the data.

For many of the fits, an automated, interactive least-squares procedure was used. The error in peak positions is estimated to be ±0.2 meV for peaks that are well resolved (for instance, the optical phonons at around 50 to 60 meV). However, for the most heavily overlapped regions, near the elastic peak where five peaks were sometimes necessary to fit the data, the computer time needed for this procedure was excessive. Instead, a variety of trial fits were compared to the data, and the best fit was chosen by eye. Figure 4 shows a typical fit obtained in this manner, using the data for 7 eV incident electrons and collection at 30° off-specular along Γ to M. From the comparison process, it is estimated that the peak positions are reproducible to ±0.5 meV. The root-mean-square deviation of the chosen fit from the data was found to be less than that for the rejected trials (those with peak energies of ±0.5 meV from the selected values) for the several cases where this deviation was calculated.

The momentum transfer for each experiment was calculated using the conservation of momentum parallel to the surface:

$$k_1 = \sqrt{2mE/h} \; (\sin\theta_{out} - \sin\theta_{inc})$$

where m is the electron mass, h is Planck's constant, and θ_{out} and θ_{inc} are the angles of collection and incidence, respectively, measured with respect to the surface normal. The data are presented in reduced coordinates (units of $2\pi/a$ for Γ to K, $4\pi/a\sqrt{3}$ for Γ to M, where a is

the lattice parameter in the basal plane) that reflect the fraction of the distance to the zone boundary. The dispersion curves are given in Figure 5, along with selected calculated bulk dispersion curves of Wakabayashi et al. (Ref. 7). These curves fit their neutron scattering measurements of the bulk phonon dispersion very well, but exhibit some differences from the surface phonon dispersion, as will be discussed in section IV.

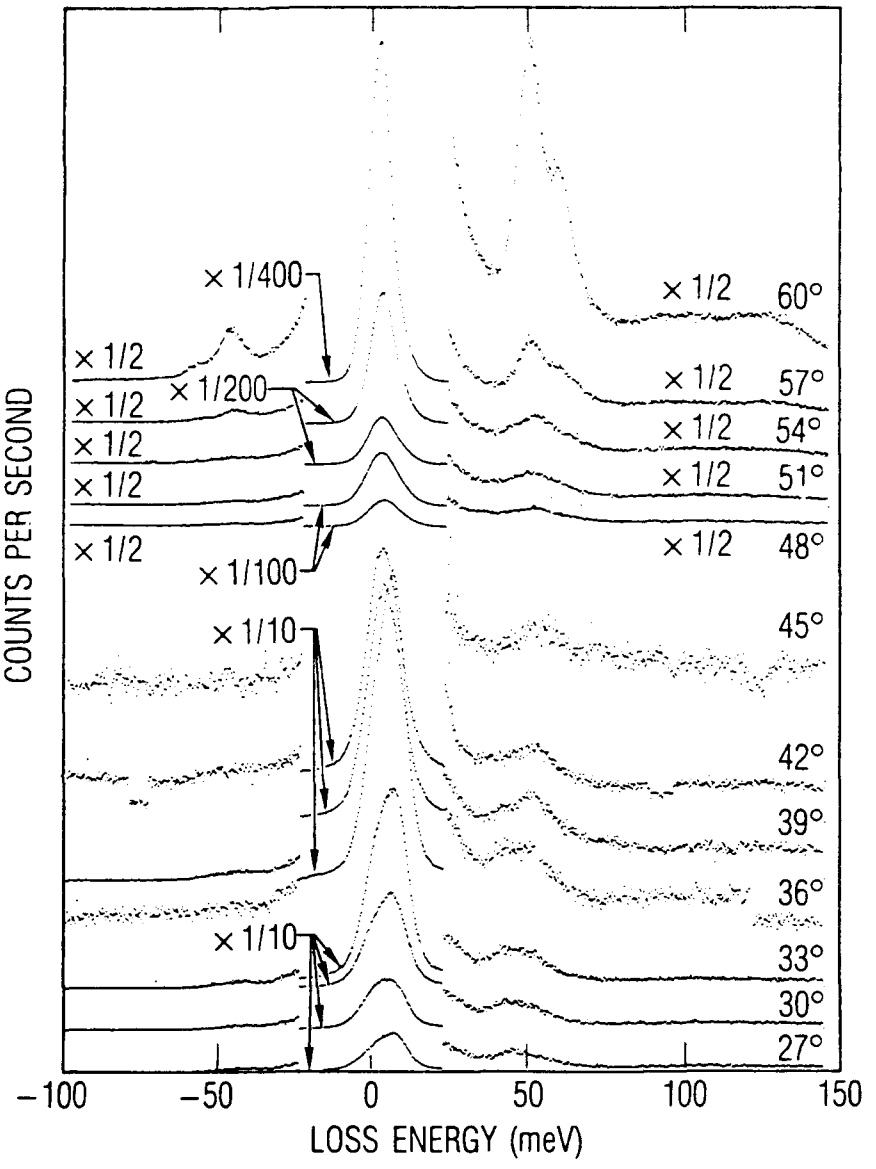

Figure 2. HREELS spectra of MoS_2 along the < 110 > azimuth (Γ to K). Incident beam energy was 15 eV. Each spectrum is labeled with the angle of collection with respect to the surface normal.

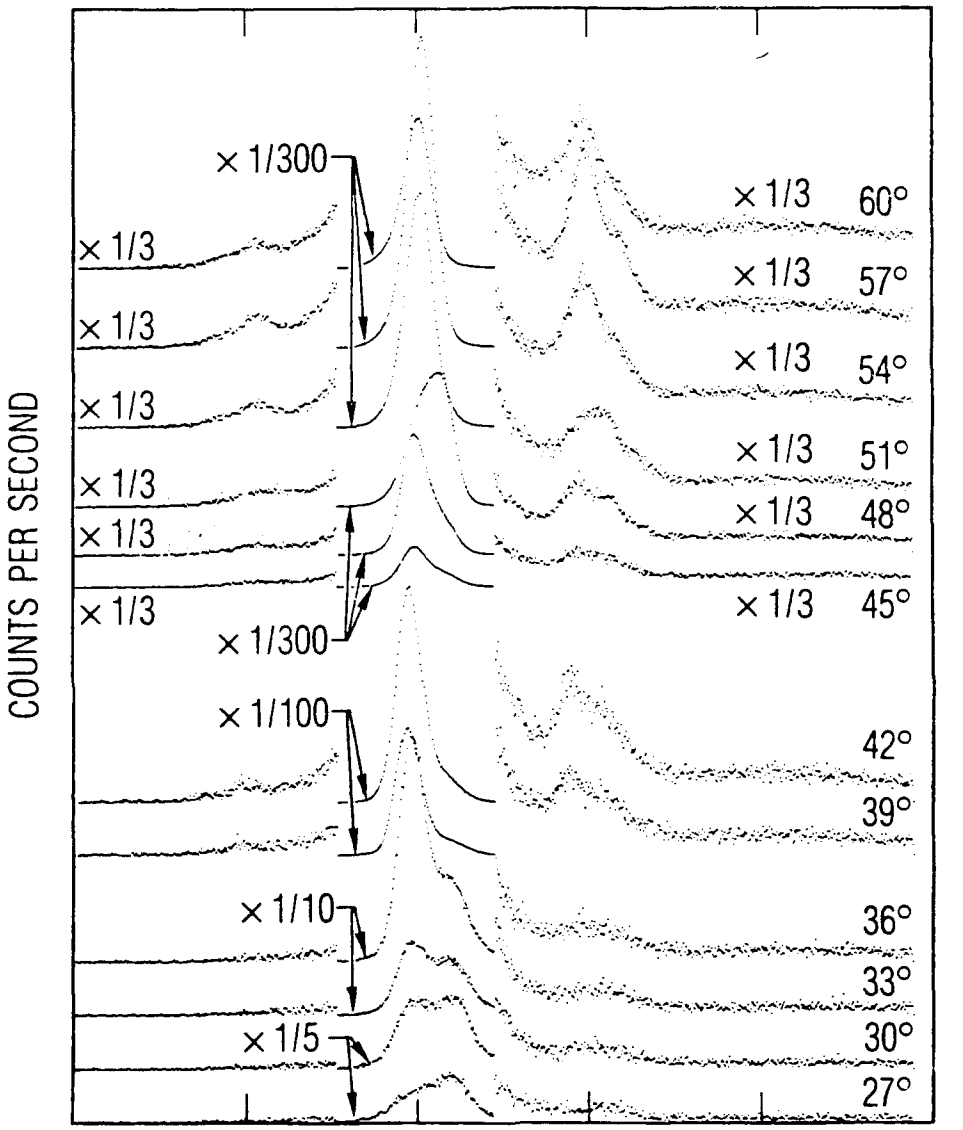

Figure 3 . HREELS spectra of MoS_2 along the <010> azimuth (Γ to M). Incident beam energy was 15 eV. Each spectrum is labeled with the angle of collection with respect to the surface normal.

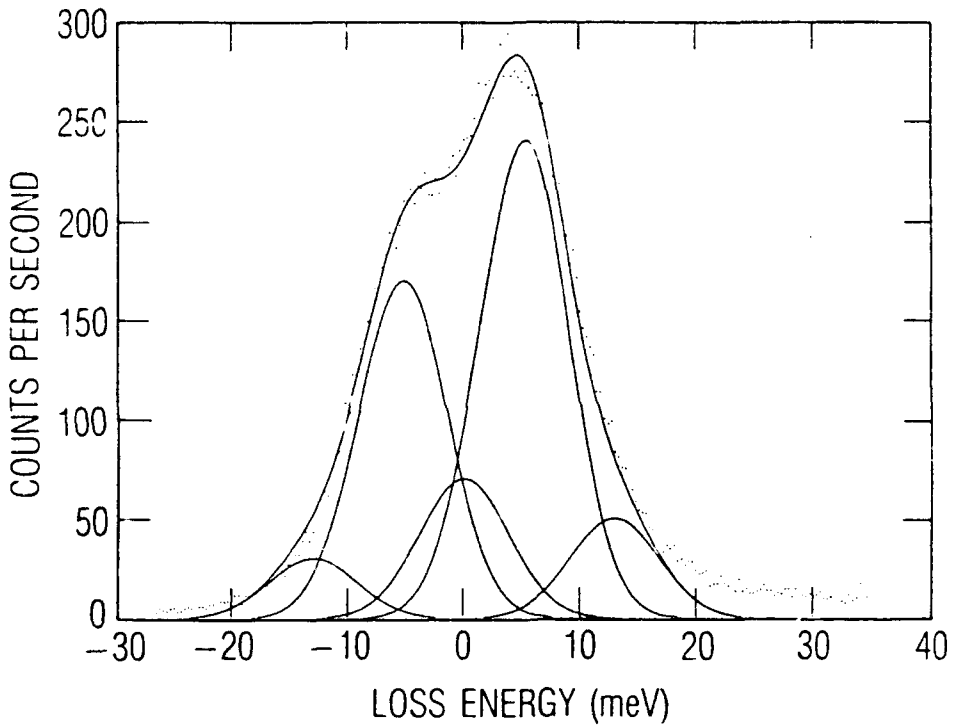

Figure 4. Example of curve fitting to HREELS spectrum of MoS_2 with 7-eV incident beam and 30° collection angle along <010> azimuth (Γ to M).

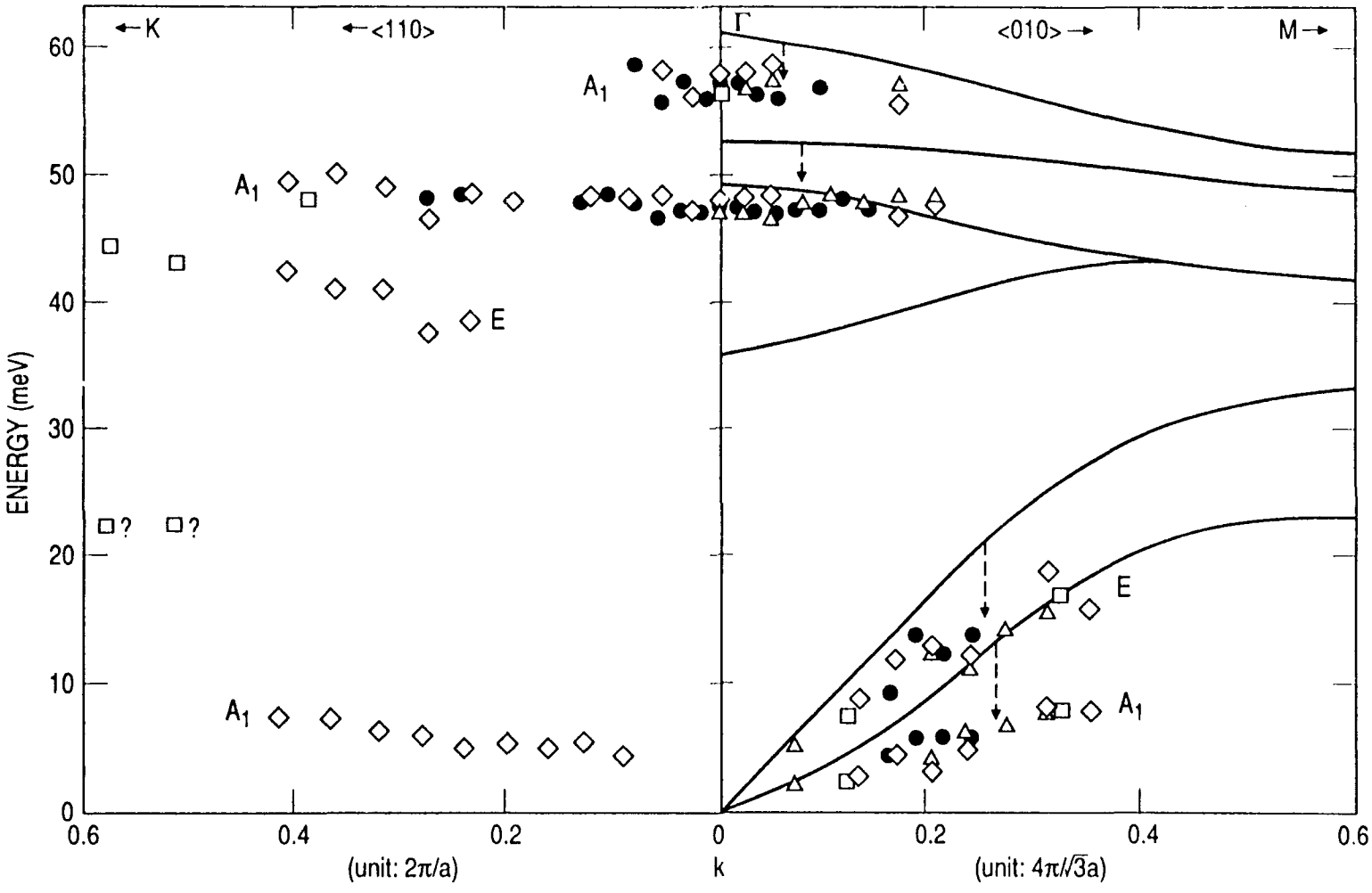

Figure 5. Surface phonon dispersion curves for MoS_2 along the <110> and <010> directions. The lines are calculated bulk curves of Wakabayashi, et al. The data points are measured for incident beam energies of 7 eV (●), 15 eV (◇), 40 eV (□, Γ to M), 30 eV (□, Γ to K), and 15 eV using a cooled sample (△).

IV. DISCUSSION

In bulk MoS_2 there are six atoms per unit cell, so 18 phonon modes are expected: 3 acoustic modes and 15 optical. At Γ the modes can be labeled by irreducible representations of the D_{6h}^4 point group ($P6_3/mmc$ space group). These modes were listed by Agnihotri et al. (Ref. 8), along with diagrams of atomic dispacements for each mode. The unit cell of the surface layer of MoS_2 has three atoms (two sulfur and one molybdenum), so 9 modes are expected: 3 acoustic modes and 6 optical modes. The point group for the surface is C_{cv}; there will be 3 A_1 modes and 3 doubly degenerate E modes. These modes are listed in Table I, with their related bulk modes (Ref. 8), atomic displacements (following Agnihotri et al.), related measured bulk phonon energies, and the surface phonon energies at Γ determined in this work.

Table I. Lattice Modes at Γ for MoS_2

IRREDUCIBLE REPRESENTATION	A_1	E	A_1	E	A_1	E
RELATED BULK IRREDUCIBLE REPRESENTATIONS (ref 8)	A_{1g} B_{1u}	E_{1g} E_{2u}	A_{2u}^2 B_{2g}^1	E_{1u}^2 E_{2g}^1	A_{2u}^1 B_{2g}^2	E_{1u} E_{2g}^2
ATOMIC DISPLACEMENTS[a]	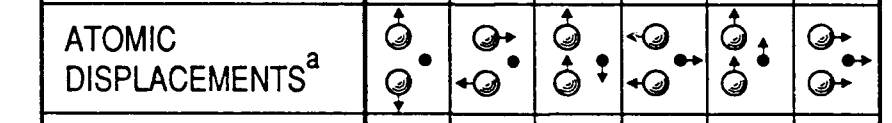					
BULK ENERGY (meV) (ref 7)	50.7	35.6	57.8	46.7	0	0
SURFACE ENERGY (meV)	47.6	–	57.2	–	0	0

[a]PROJECTED ON (110) PLANE. ◎ = S, • = Mo, <0001> DIRECTION IS TOWARD THE TOP OF THE PAGE

The HREELS peaks measured in these experiments can be assigned to the expected surface phonon modes. Two of the A_1 modes are optical and will be dipole-active vibrations. These should be observed in specular reflection, and should decrease in intensity as the elastic peak decreases in intensity when scattering is detected off-specular. The peaks at 47.6 and 57.2 meV behave in this manner, so they are assigned as A_1.

There are two E optical modes, which are in-plane vibrations and could be excited by the impact scattering mechanism that dominates HREELS experiments away from the specular direction. For our experimental geometry, the observed impact modes must be totally symmetric with respect to the scattering plane. These two modes would then be visible in the $<110>$ direction, and along this azimuth we have a peak in the spectra for $k \geq 0.2$. The E modes should not be visible along the $<010>$ direction, and as expected we find no corresponding peak in the spectra. The energy of the peak found along the $<110>$ direction is not listed in Table I because it was not measured at Γ.

Acoustic modes approach 0 meV as k approaches 0. We expect an A_1 mode (the Rayleigh wave) to be the lowest energy vibration, and assign the lowest energy peak in the spectra to this mode. The acoustic E mode is present only along the $<010>$ azimuth.

At $k = 0.5$ to 0.6 along the $<110>$ azimuth, two peaks with very low signal to noise are found. The assignment of these peaks is unclear.

The energies of the surface phonons are less than those of the related bulk phonons. The A_1 optical modes are 0.6 and 3.1 meV lower in energy (experimental error ± 0.2 meV), with a similar dispersion to the bulk modes. The two E optical modes are probably degenerate, since we only observe one peak in the spectra that we can assign to modes of this type. They must also be lower in energy than their related bulk modes, which were not measured along Γ to K, since Rayleigh's theorem states that if the spring constant of one vibration in a set of harmonically coupled masses is lowered, all the vibrational frequencies must decrease. The energies of the acoustic modes measured here are generally 30%–50% lower than those of the bulk acoustic modes measured by Wakabayashi et al. (Ref. 7) across the Brillouin zone. These differences are larger than our estimated experimental error (± 0.5 meV).

The large softening of the surface phonons with respect to the bulk phonons is similar to the case for GaSe, and different from that of graphite. The optical phonons in GaSe were also softened by several percent. The explanation advanced for GaSe surface phonon softening could also be viable for MoS_2: increased S polarizability at the surface, and increased van der Waals attraction at the first gap. This explanation is also supported by the LEED results, indicating a contraction of the first van der Waals gap in MoS_2.

V. CONCLUSIONS

The dispersion of the surface phonons of MoS_2 has been measured by HREELS along both the <010> and <110> azimuths (Γ to K and Γ to M). The surface phonons are lower in energy than the corresponding bulk phonons, as was found in previous studies of GaSe. The contraction of the first van der Waals gap in MoS_2 as measured by LEED, combined with the softer surface phonons measured in these experiments, suggests that the S atoms at the surface may be more polarizable than those in the bulk, as seems to be the case for the surface Se atoms in GaSe.

REFERENCES

1. B. J. Mrstik, R. Kaplan, T. L. Reinecke, M. Van Hove, and S. Y. Tong, *Phys. Rev. B* **44**, 897 (1977).

2. J. L. Wilkes, R. E. Palmer, and R. F. Willis, *J. Elect. Spectr. and Relat. Phenom.* **44**, 355 (1987).

3. C. Oshima, T. Aizawa, R. Souda, Y. Ishizawa, and Y. Sumiyoshi, *Solid State Comm.* **65**, 1601 (1988).

4. R. Nicklow, N. Wakabayashi, and H. G. Smith, *Phys. Rev. B* **5**, 4951 (1972).

5. G. Brusdeylins, R. Rechsteiner, J. G. Skofronick, J. P. Toennies, G. Benedek, and L. Miglio, *Phys. Rev. B* **34**, 902 (1986).

6. J. C. McMenamin and W. E. Spicer, *Phys. Rev. B* **16**, 5474 (1977); J. Bandet, A. Malvand, and Y. Quemener, *J. Phys. C* **13**, 5657 (1980).

7. N. Wakabayashi, H. G. Smith, and R. M. Nicklow, *Phys. Rev. B* **12**, 659 (1975).

8. O. P. Agnihotri, H. K. Sehgal, and A. K. Garg, *Solid State Commun.* **12**, 135 (1973).

TECHNOLOGY OPERATIONS

The Aerospace Corporation functions as an "architect-engineer" for national security programs, specializing in advanced military space systems. The Corporation's Technology Operations supports the effective and timely development and operation of national security systems through scientific research and the application of advanced technology. Vital to the success of the Corporation is the technical staff's wide-ranging expertise and its ability to stay abreast of new technological developments and program support issues associated with rapidly evolving space systems. Contributing capabilities are provided by these individual Technology Centers:

Electronics Technology Center: Microelectronics, solid-state device physics, VLSI reliability, compound semiconductors, radiation hardening, data storage technologies, infrared detector devices and testing; electro-optics, quantum electronics, solid-state lasers, optical propagation and communications; cw and pulsed chemical laser development, optical resonators, beam control, atmospheric propagation, and laser effects and countermeasures; atomic frequency standards, applied laser spectroscopy, laser chemistry, laser optoelectronics, phase conjugation and coherent imaging, solar cell physics, battery electrochemistry, battery testing and evaluation.

Mechanics and Materials Technology Center: Evaluation and characterization of new materials: metals, alloys, ceramics, polymers and their composites, and new forms of carbon; development and analysis of thin films and deposition techniques; nondestructive evaluation, component failure analysis and reliability; fracture mechanics and stress corrosion; development and evaluation of hardened components; analysis and evaluation of materials at cryogenic and elevated temperatures; launch vehicle and reentry fluid mechanics, heat transfer and flight dynamics; chemical and electric propulsion; spacecraft structural mechanics, spacecraft survivability and vulnerability assessment; contamination, thermal and structural control; high temperature thermomechanics, gas kinetics and radiation; lubrication and surface phenomena.

Space and Environment Technology Center: Magnetospheric, auroral and cosmic ray physics, wave-particle interactions, magnetospheric plasma waves; atmospheric and ionospheric physics, density and composition of the upper atmosphere, remote sensing using atmospheric radiation; solar physics, infrared astronomy, infrared signature analysis; effects of solar activity, magnetic storms and nuclear explosions on the earth's atmosphere, ionosphere and magnetosphere; effects of electromagnetic and particulate radiations on space systems; space instrumentation; propellant chemistry, chemical dynamics, environmental chemistry, trace detection; atmospheric chemical reactions, atmospheric optics, light scattering, state-specific chemical reactions and radiative signatures of missile plumes, and sensor out-of-field-of-view rejection.